

# Power Flow Analysis of MMC-HVDC System with Margin Voltage and Voltage Droop Control Strategies

Maxwel da Silva Santos\*, Luciano Sales Barros\*\*,  
Rafael Lucas da Silva França\*, Flavio Bezerra Costa\*, Kai Strunz\*\*\*.

\* Federal University of Rio Grande do Norte, Natal-RN, Brazil

\*\* Federal University of Paraíba, João Pessoa-PB, Brazil

\*\*\* Technische Universität Berlin, Germany

e-mails: maxwel@ufrn.edu.br, lsalesbarros@ci.ufpb.br,  
rafaellucas@ufrn.edu.br, flaviocosta@ect.ufrn.br, kai.strunz@tu-berlin.de

---

**Abstract:** High voltage direct current (HVDC) systems are an alternative for transmission of energy with higher efficiency and lower electrical losses over long distances. HVDC systems have become more common with the evolution of power electronics, promoting the interest of research in power flow control techniques. The main objective of this paper is to perform evaluations of the power flow in a meshed multi-terminal HVDC (MT-HVDC) system based on the multilevel modular converter (MMC). Two different control strategies were considered; The margin voltage; and the voltage droop strategies. Two assessment scenarios were considered: when an active power reference takes place in the system; and when a DC transmission line is open-circuit due to a failure in the DC grid. For both of these test cases, the system with the margin voltage control obtained a new balance of power flow with less oscillations in power and voltage than the one with the voltage droop control.

**Keywords:** Multi-Terminal High Voltage Direct Current; Margin Voltage Control; Modular Multilevel Converter; Voltage Droop Control; Voltage Source Converter.

---

## 1. INTRODUCTION

High voltage direct current systems are an alternative for connecting asynchronous AC grids and for the transmission of large blocks of energy over long distances mainly because HVDC lines have neither reactive losses nor skin effect (Ackermann, 2002). Therefore, HVDC lines suffer less losses and have smaller diameters, which reduces its cost compared to AC lines for long distances (Ackermann, 2002). In order to improve the reliability of renewable energy integration and the management of energy flow from offshore production, such as the production of offshore wind farms (OWF), to onshore transport, the MT-HVDC grid concept has been introduced (Rekik et al, 2018)-(Saburg et al, 2020). It performs the connection of the OWF with the onshore AC system by means of multiple HVDC transmission lines.

High voltage direct current grids based on voltage-source converters (VSC) have the advantage of the independent control of active and reactive power and no need for reversing the voltage polarity to change power direction (Saburg et al, 2020). The MMC offers advantages when compared to the VSC such as high scalability, low switching losses, better output voltage waveform, and no requirement for a common DC-link capacitor (Saburg et al, 2020) - (Gemmell et al, 2008). Besides, the MMC generates a voltage harmonic content smaller than the one generated by the VSC, thus reducing the values of reactive components of the filter, which can even be eliminated in some cases. In addition, when a large number of switching modules (SMs) is used, the switching frequency of the SM is reduced and the MMC switching losses are

minimized (Martinez-Rodrigo et al, 2017). The MMC with half-bridge submodules has been established as the dominant topology for HVDC systems because the full-bridge submodules compared to the half-bridge submodule configuration requires twice the number of semiconductor switches, resulting in higher initial cost and losses (Ahmed et al, 2015).

In MT-HVDC grids, the power sharing is achieved by regulating the DC voltage at VSCs. Therefore, at least one of the VSCs of MT-HVDC grid must regulate the DC voltage and the control system of the other VSCs must regulate the power flows to terminals in order to ensure that the power is transferred with the best possible efficiency. The control system also must maintain the system running even under certain failures and abnormal conditions, such as power flow variations and open-circuit of a DC transmission line. In the first case, the power flow of the respective MMC will follow the reference changing its DC voltage value, thus maintaining the correct operation of the DC grid. In the second case, in order to maintain the same power flow in between MMCs, the DC voltages in terminals are readjust for to change the power flow in the other lines in operation, maintaining the power flow between the MMCs.

This paper evaluates the performance of two control methods, which are the margin voltage and voltage droop controls, when applied in the MT-HVDC system with MMC under two challenging abnormal conditions, power flow variation and open-circuit of a DC transmission line. A four-terminal MT-HVDC system with meshed topology based on

the MMC of five switching modules (SMs) per arm of the half-bridge topology was implemented in this paper. In the DC side of system, the MMCs operate as VSC and are interconnected by five DC transmission lines of the monopolar topology with metal return. In the AC side, The MT-HVDC system interconnects four distinct AC systems, one OWF and three onshore AC grids. Dynamic models of MMCs and their control systems as well as the DC and AC grid models have been implemented. The integration of these models in MATLAB/Simulink has been carried out, constituting a platform of simulation of MT-HVDC system based on MMC.

This paper is organized according to the following structure: Section 2 presents the model of MMC and their control systems. Section 3 presents the control strategies of MT-HVDC. Section 4 presents the tested MT-HVDC system. Section 5 presents simulation results and their analysis. At the end, the conclusions are presented.

## 2. MODULAR MULTILEVEL CONVERTER

This section defines the MMC model, modulation technique for SMs switching control and balancing of capacitor voltages.

### 2.1 Converter Model

A simulation model for the MMC is shown in Fig. 1. The converter consists of six arms, which each one contains a series connection of five SMs and an inductor  $L_{arm}$  and a resistance  $R_{arm}$ . Each SM contains a half-bridge of two IGBTs and a capacitor  $C_{sm}$ .

The voltage of the capacitor  $C_{sm}$  is given by  $V_c = V_{dc}/5$ , where  $V_{dc}$  is the nominal DC-link voltage of MMC.  $V_c$  is influenced by the phase current, which flows through the AC three-phase load. Each SM can be toggled between two different states: the ON-state, when the upper IGBT is switched on and the lower one is switched off; the OFF-state, when the lower IGBT is switched on and the upper one is switched off. Therefore, SM terminal voltage will be  $V_{sm}(t) = V_c$  in the ON-state and  $V_{sm}(t) = 0$  in the OFF-state.

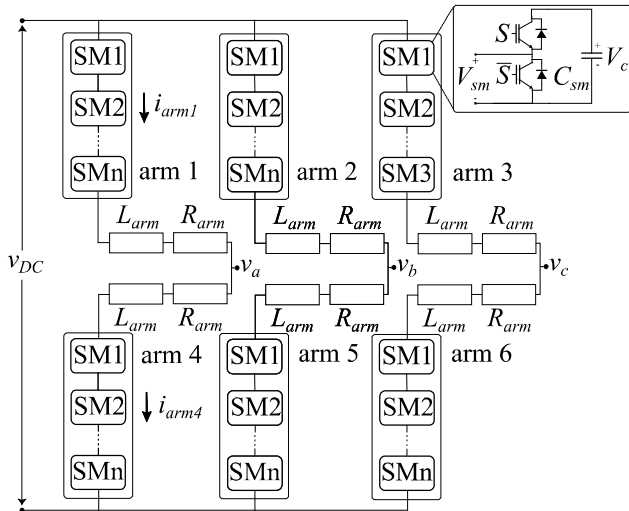


Figure 1: MMC model scheme.

The DC side is connected to the DC-link of the MT-HVDC. The three-phase AC side is modeled by the AC voltage

source,  $V_g$ , and an equivalent impedance of the AC grid and the coupling transformer.

### 2.2 Phase Disposition-Sinusoidal Scalar Pulse Width Modulation

Phase disposition-sinusoidal scalar pulse width modulation (PD-SPWM) is a scalar pulse width modulation (SPWM) similar to the one used in a classic two level inverter, but adapted to the case of multilevel converters (Martinez-Rodrigo et al, 2017). A high-frequency (carrier) triangle signal is compared to a low-frequency (modulator) signal to produce the output voltage. According to the offset between the carriers, there are several types of modulation (Martinez-Rodrigo et al, 2017). The SPWM modulation used in this paper is the PD-SPWM, in which the offset between the carriers is null, as shown in Fig. 2.

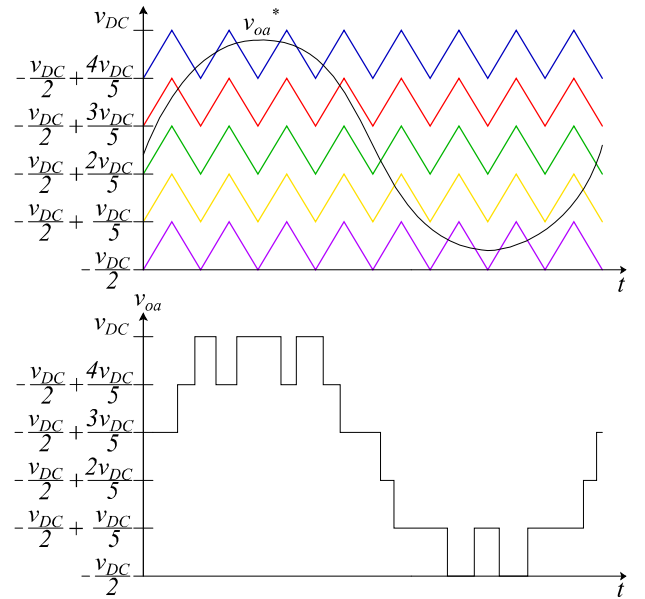


Figure 2: PD-SPWM scheme. Based on (Martinez-Rodrigo et al, 2017).

### 2.3 Balancing of Capacitor Voltages

The capacitors of the SMs change their voltage depending on the current flowing through the SMs, but the voltages of the SMs should be kept approximately equal to the theoretical  $V_{dc}/5$  (Martinez-Rodrigo et al, 2017). Otherwise, the capacitor voltages of the SMs will become increasingly unbalanced. Thus, eventually the AC voltage output cannot be controlled. Therefore, the SM voltages must be measured and the appropriate actions must be taken to maintain the SM voltages at their nominal value.

Different algorithms can be used to balance capacitor voltages of the SMs. The most commonly used algorithm measures voltages of capacitors and chooses the SMs that must be ON depending on the direction of the current (Rohner, 2010). In each arm of the MMC, the SMs that must be set to ON are chosen according to the own arm current direction,  $i_{arm}$ . When  $i_{arm}$  is positive, i.e., when current flows from the DC grid to the AC grid, SMs that have less voltage are turned ON to charge. Otherwise, when  $i_{arm}$  is negative, the SMs that have the highest voltages are turned ON to discharge.

### 3. CONTROL OF VOLTAGE SOURCE CONVERTERS FOR MT-HVDC

This section defines the control strategies used in this work. The margin voltage and voltage droop control techniques consist of two control meshes: inner and outer loops. The inner control loop focuses on regulating the converter currents, where as the outer control loop aims to fill other objectives as voltage or power regulation. Balanced voltages are assumed in these schemes.

#### 3.1 Inner Control Loop

The inner control loop system show in Fig. 3 is common to both margin voltage and voltage droop control strategies. In the converter the connection with the AC grid is made with a three-phase RL impedance. Applying inverse transformation of clark, for  $\theta = \theta_g$ , where  $\theta_g$  is the AC grid voltage angle obtained through of a Phase-Lag Locker (PLL), the grid-connection dq model is given by (Barros and Barros, 2017) - (Santos and Barros, 2019):

$$v_d^g = R_{arm}i_d^g + L_{arm} \frac{di_d^g}{dt} - \omega_g L_{arm} i_q^g + V_g \quad (1)$$

and

$$v_q^g = R_{arm}i_q^g + L_{arm} \frac{di_q^g}{dt} + \omega_g L_{arm} i_d^g, \quad (2)$$

where  $v_d^g$  and  $v_q^g$  are voltages in dq frame at the output of the converter;  $i_d^g$  and  $i_q^g$  are currents in dq frame at the impedance of the converter;  $\omega_g$  is the grid frequency;  $\omega_g L_{arm} i_q$  ( $e_{sd}$ ) and  $\omega_g L_{arm} i_d$  ( $e_{sq}$ ) are the cross coupling terms.

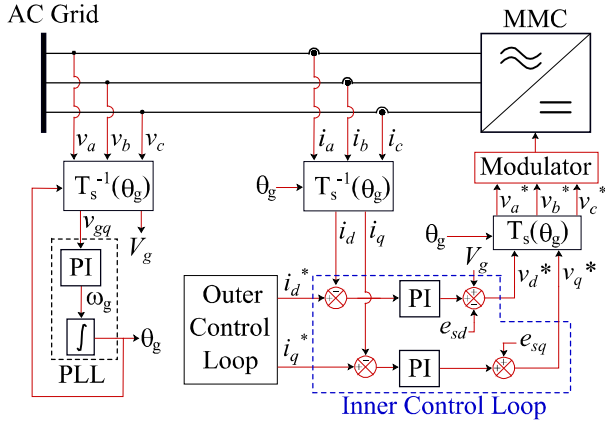


Figure 3: Inner control loop scheme.

#### 3.2 Margin Voltage Outer Control Loop

In master-slave scheme, only one converter, named master station, is responsible by the DC voltage regulation of the entire grid, while other of converters, named slave stations, are responsible for the power flow regulation of the grid (Rekik, 2018). Therefore, the master station works in constant voltage mode and slave stations are configured in constant power mode.

The margin voltage control scheme has been proposed to improve reliability by sharing the responsibility for regulating the voltage among two or more terminals. Basically, the margin voltage scheme is a master-slave one. However, it has

one or more back-up master stations capable of taking over the voltage regulation in case of outage of the main master.

In margin voltage, the master converter works in constant voltage mode and the rest of converters are configured in constant power mode, as at or mentored. However, when outages of the main master occurs, the back-up master converter leaves the constant power mode and starts in the constant voltage mode.

In the  $\theta_g$  reference, the active and reactive power, delivered in the AC grid are given by (Santos and Barros, 2019):

$$P_g^g = V_g i_d^g \quad (3)$$

and

$$Q_g^g = -V_g i_q^g, \quad (4)$$

thus, the active and reactive power can be controlled, respectively, with components of direct axis,  $i_d$ , and quadrature axis,  $i_q$ , of the current delivered to the AC grid.

Fig. 4 depicts the constant power control scheme, which includes a PI controller and the factor  $1/V_g$  in order to ensure the power delivered to the DC side is maintained at  $P_g^*$ .

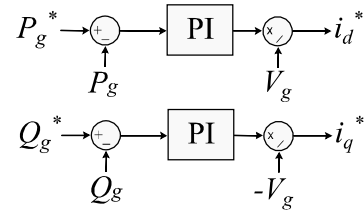


Figure 4: Constant power control scheme.

The DC link voltage,  $V_{DC}$ , is obtained as follows:

$$C \frac{dV_{DC}}{dt} = \frac{P_{DC} - P_g}{V_{DC}}, \quad (5)$$

where  $C$  is the capacitance of the DC link;  $P_{DC}$  is the power from the DC grid;  $P_g$  is the output power of the MMC.

Fig. 5 depicts the constant voltage control scheme, which includes a PI controller in order to ensure the voltage to the DC side is maintained at  $v_{DC}^*$ .

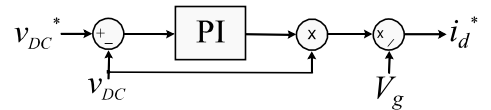


Figure 5: Constant voltage control scheme.

#### 3.3 Voltage Droop Outer Control Loop

The droop control is a proportional control aimed for regulating the DC-link voltage (Rekik et al, 2018). The droop control law can act directly on the current current or constant power control input. The droop gains are computed according to the maximum allowed voltage deviations for given power changes.

The voltage droop control consists of two or more stations equipped with droop control and the rest of stations with constant power control. In droop control, the responsibility for the DC voltage regulation is shared among all stations with

droop control. As a consequence, in case of an outage of one terminal, the rest of the system is able to continue working. Besides, since all terminals with droop control participate in the voltage and power regulation, large power balances can be managed with stations of small power rating. Fig. 6 depicts the voltage droop control scheme.

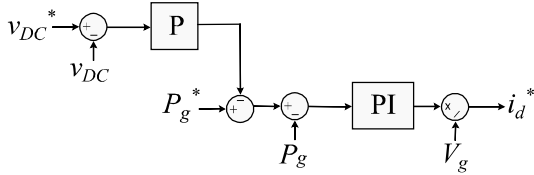


Figure 6: Voltage Droop control scheme.

### 3.3 Controller Design

In this paper, the parameters  $K_p$  and  $K_i$ , used in the controllers of the current inner loop and the active and reactive power outer loop for the margin voltage and voltage droop are the same. The control parameters are shown in the Appendix.

## 4. MULTITERMINAL HIGH VOLTAGE DIRECT CURRENT SYSTEM

The MT-HVDC system based on MMC shown in Fig. 7 was first proposed in Leterme et al, (2015). It consists of four stations based on MMCs with five SMS per arm of the half-bridge topology. The AC systems are modeled by an AC voltage source with constant frequency and amplitude in series with the equivalent impedance of the grid and coupling transformer. In the DC side there are five monopolar cables with metal return. The current limiting reactors,  $L_r$ , are placed at each DC line terminal. The studied system adopts the symmetric monopole configuration. The grid and converter parameters are shown in the Appendix.

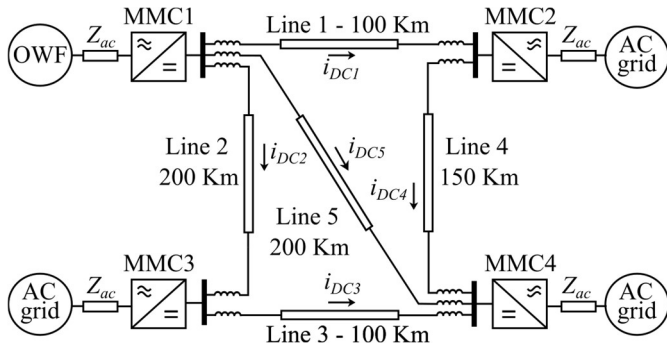


Figure 7: Single line diagram of the MT-HVDC system. Based on (Leterme et al, 2015).

## 5. SIMULATION RESULTS

Performance analyzes of the MMC-based MT-HVDC system with margin voltage and voltage droop control strategies for two cases are accomplished with simulations. In the steady-state, the MMC 1 and MMC 2 deliver -200 MW and -100 MW active power flow (power flow from AC grid to DC grid), respectively, and the MMC 3 and MMC 4 deliver 150 MW active power flow each (power flow from DC grid to AC grid). The references of reactive power of all MMCs are zero throughout the simulation. The first studied case considers a variation in the active power reference of the MMC 2 control

system, where the active power reference varies linearly from -100 MW to 75 MW lasting 0.5 seconds. The second studied case considers an open-circuit in the fourth DC transmission line (line 4), where the transmission line operates normally and in 7 seconds of simulation the both line terminals are opened due to a fault.

### 5.1 Active Power Reference Variations

Figs. 8 to 10 depict the performance of the MT-HVDC system when subjected to a variation in the active power reference of the MMC 2 control system, where Fig. 8 depicts the active power flows of the MMCs. For the margin voltage control, the variation in active power flow of MMC 2 causes a variation in active power flow of MMC 4 because only the main station can vary its active power flow to ensure power balance in the DC grid, while for the voltage droop control, the variation in active power flow of MMC 2 causes variations in active power flow of MMC 3 and MMC 4 because only the stations equipped with droop control can vary their power flows to ensure power balance in the DC grid. Fig. 9 depicts the DC grid voltages, which present voltage variations in order to ensure balance. Fig. 10 depicts the DC currents in the DC lines.

In the first case, the MT-HVDC system with the margin voltage control system performed better than with the voltage droop control because the transients were faster and with less oscillations due to having a terminal ensuring tight regulation of DC voltage.

### 5.2 Open-Circuit in the DC line

Figs. 11 to 13 depict the performance of the MT-HVDC system when submitted to an open-circuit in the DC transmission line 4, where line terminals are opened due to a failure. Therefore, the line operation is interrupted and the direct connection between the terminals MMC 2 and MMC 4 is broken. Fig. 11 depicts the active power flow of the MMCs. For margin voltage and voltage droop controls, variations occur on the active power flows of the MMCs due to opening of DC transmission line 4. However, the power flows return to their steady-state values with similar performances for the two system controls. Fig. 12 depicts the DC grid voltages. Regarding the margin voltage, the DC voltage of master station does not vary. However, the DC voltages of other stations vary in order to keep active power flows constant between stations, while for voltage droop, all DC voltages vary in order to keep active power flows constant between stations. Fig. 13 depicts the DC currents in the DC lines, where variations in the DC line currents occur due to variations in DC-link voltages, in order to keep active power flows constant.

In the second case, the MT-HVDC system with margin voltage control presented a similar performance compared to the system with voltage droop control. Although the transients in active power flows and currents of the DC transmission lines with margin voltage control were slower, it presented less oscillations and the transient at DC voltages were faster and with less oscillations due to there is a tight regulation of DC voltage.

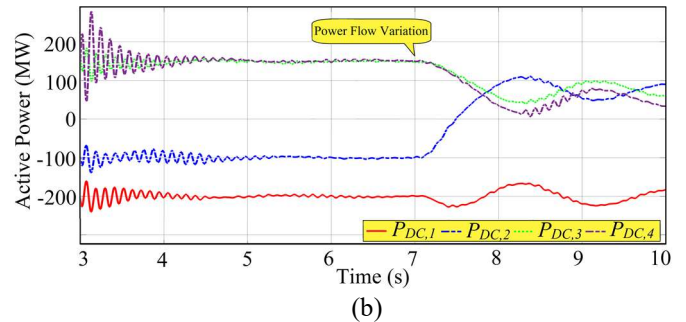
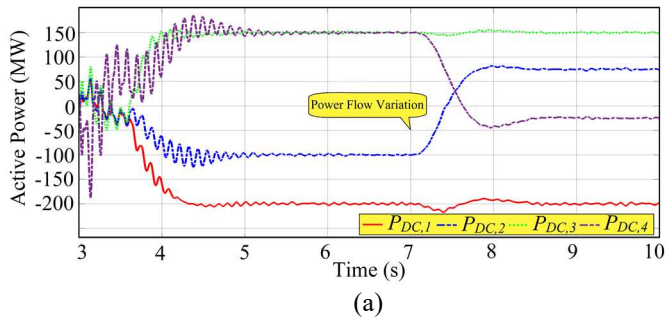


Figure 8: Active power flows for active power variations case: (a) margin voltage control; (b) voltage droop control.

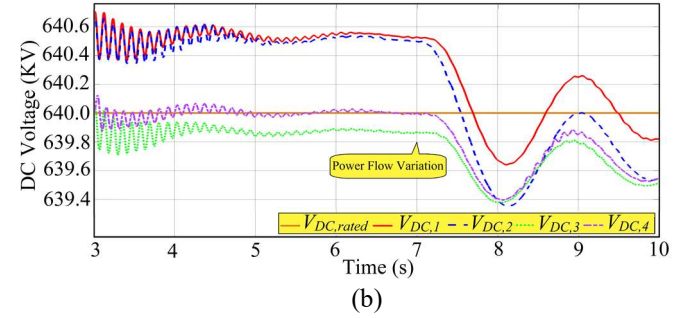
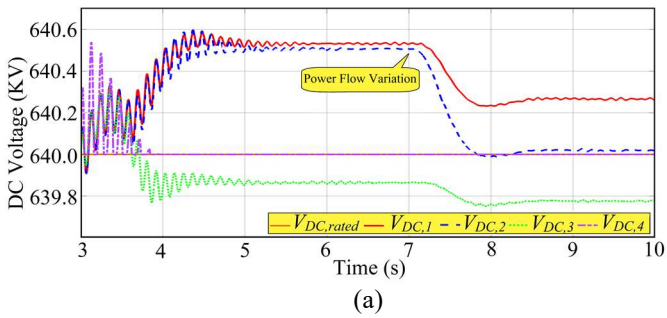


Figure 9: DC-link voltages for active power variations case: (a) margin voltage control; (b) voltage droop control.

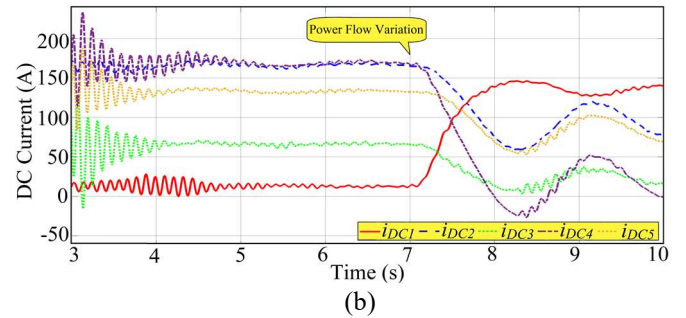
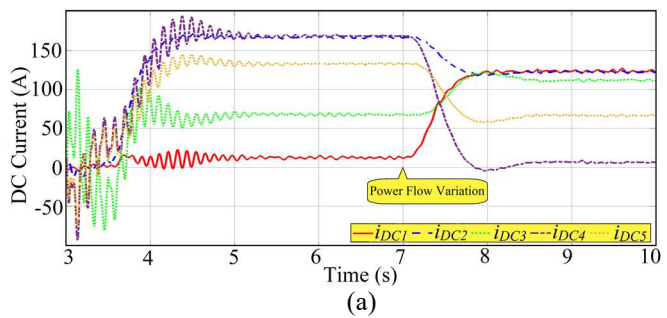


Figure 10: Currents in DC lines for active power variations case: (a) margin voltage control; (b) voltage droop control.

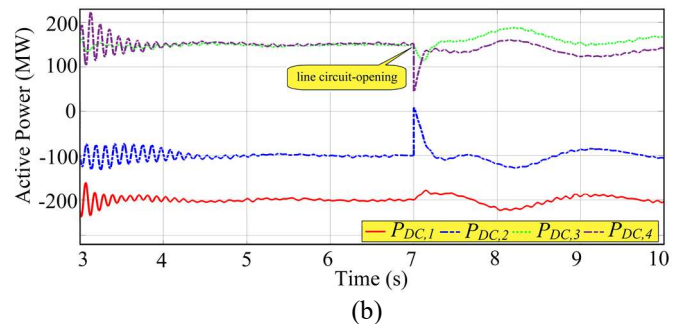
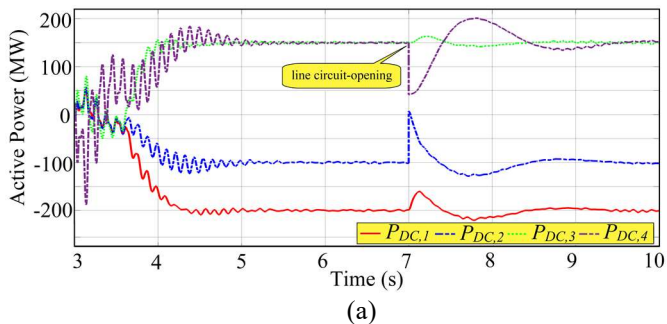


Figure 11: Active power flows for line open-circuit case: (a) margin voltage control; (b) voltage droop control.

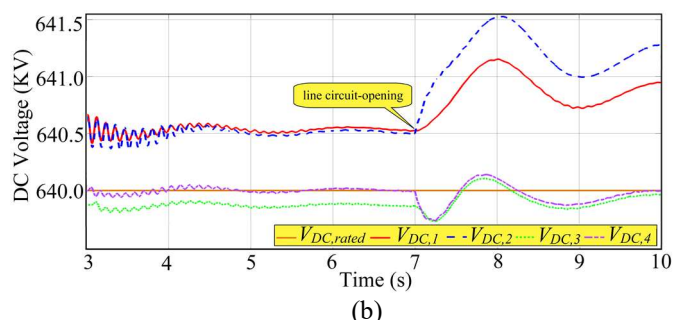
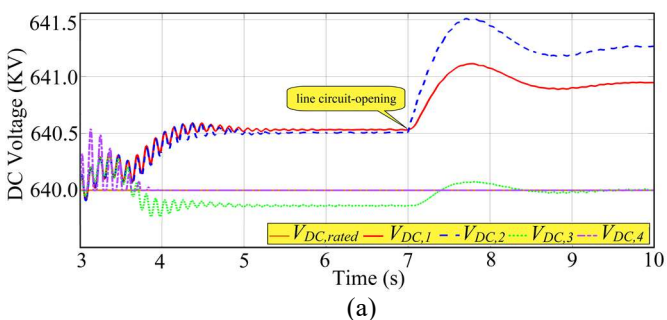


Figure 12: DC-link voltages for line open-circuit case: (a) margin voltage control; (b) voltage droop control.

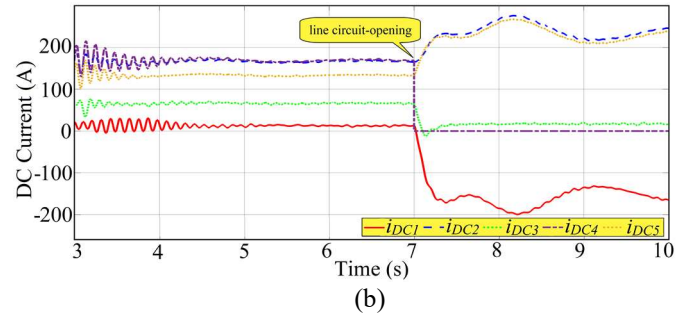
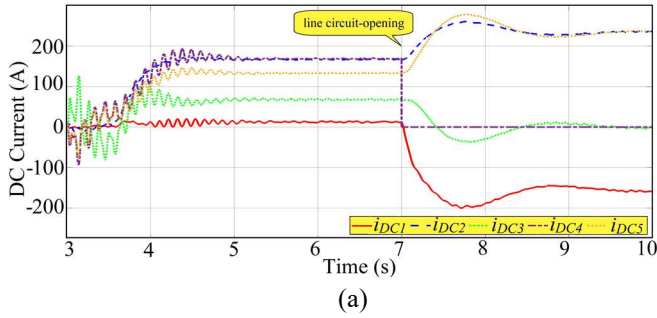


Figure 13: Currents in DC lines for line open-circuit case: (a) margin voltage control; (b) voltage droop control.

## 6. CONCLUSIONS

This paper presented the performance evaluation of margin voltage and voltage droop control strategies based in MT-HVDC grids considering variations in active power flows and open-circuit in the DC transmission line.

The margin voltage control presented the lowest oscillations in the active power and in the DC voltage because the number of stations participating in the energy balance is lower than in the voltage droop control. However, since only the main station terminal participates in the energy balance, the master converter requires a higher power so in order to ensure the power balance. Therefore, the energy balance management is lower compared to voltage droop control. In the droop control, all terminals equipped with droop control participate in the energy balance, which ensure that large power balances can be managed with low power stations.

The  $K_p$  value in the droop control directly influences the voltage and power oscillations. The higher the  $K_p$  value, the faster the system response. However, a very high  $K_p$  value can generate large oscillations in system voltages and power flows, which is undesirable. Therefore, to choose the margin voltage control, the maximum energy balance supported by the system must be considered. In turn, to choose the voltage droop, the levels of oscillations supported by the system must be considered.

The margin voltage obtains a better performance because having the master terminal ensure tight regulation of DC voltage. Therefore, a more precise control of the power flow can be achieved.

## ACKNOWLEDGMENT

This work was supported by the National Council for Scientific and Technological (CNPq) and by the Coordination for the Improvement of Higher Education Personnel (CAPES), Brazil.

## APPENDIX

The Control parameters data are presented in Table 1 and MT-HVDC system data are presented in Table 2.

Table 1: Control Parameters

Parameters	Margin Voltage	Voltage Droop
$K_i$ inner loop	200	200
$K_p$ inner loop	20	20
$K_i$ outer loop	4	4
$K_p$ outer loop	0.2	0.2
$K_p$ droop	-	30000

Table 2: MT-HVDC Grid Parameters

Parameters	Value	Unit
AC grid voltage $V_{ac}$	370	kV
AC grid inductance $L_{ac}$	400	$\mu$ H
AC grid resistance $R_{ac}$	10	m $\Omega$
DC grid voltage $V_{dc}$	$\pm 320$	kV
DC line resistance $R_{dc}$	10	m $\Omega$ /km
Current limiting reactor $L_r$	10	mH
Sub-module capacitance $C_{sm}$	10	mF
Arm inductance $L_{arm}$	50	mH
Arm resistance $R_{arm}$	10	m $\Omega$

## REFERENCES

- Ackermann, T., (2002). Transmission systems for offshore wind farms. *IEEE Power Engineering Review*, Vol. 22, no. 12, pp. 23-27.
- Ahmed, N., Angquist, L., and Mahmood et al., S., (2015). Efficient modeling of an MMC-based multiterminal DC system employing hybrid HVDC breakers, *IEEE Trans. Power Deliv.*, vol. 30, no. 4, pp. 1792-1801.
- Barros, L. S., and Barros, C. M. V., (2017). Modified Grid-Side Control of PMSG-Based Wind Generators to Extend Withstand Voltage Sags, *Power Electronics*, vol. 22, no. 2, pp. 167-178.
- Gemmell, B., Dorn, J., Retzmann, D. and Soerangr, D., (2008). Prospects of multilevel VSC technologies for power transmission, *Transmission and Distribution Conference and Exposition*. pp. 21-24.
- Leterme, W., Ahmed, N., Beerten, J., Angquist, L., Hertem, D.V. and Norrga, S., (2015). A new HVDC grid test system for HVDC grid dynamics and protection studies in EMT-type software, *IET International Conference on AC and DC Power Transmission*, Birmingham, pp. 1-7.
- Martinez-Rodrigo, F., Ramirez, D., Rey-Boue, A. B., Pablo S. and Lucas, L. C. H., (2017). Modular Multilevel Converters: Control and Applications. *Energies*, Vol. 10.
- Rekik, A., Boukettaya, G. and Kallel, R., (2018). Comparative study of two control strategies of a Multiterminal VSC-HVDC systems, *Proc. 7th Int. Conf. Syst. Control*, pp. 366-371.
- Rohner, S., Bernet, S., and Hiller et al., M., (2010). Modulation losses and semiconductor requirements of modular multilevel converters, *IEEE Trans. Ind. Electron.*, vol. 57, no. 8, pp. 2633-2642.
- Saburg Jr., L. A., Musa, A. A., Costa, F. B., and Monti, A. A., (2020). Real-time boundary wavelet transform-based DC fault protection system for MTDC grids, *Electrical Power and Energy Systems*, Vol. 115.
- Santos, M. S., and Barros, L. S., (2019). Offshore Wind Energy Conversion System Based on Squirrel Cage Induction Generator Connected to the Grid by VSC-HVDC Link." *Innovative Smart Grid Technologies Conference - Latin America (ISGT LA)*. pp. 15-18.